Inorganic Chemistry

Article

pubs.acs.org/IC

Anion Receptor Design: Exploiting Outer-Sphere Coordination Chemistry To Obtain High Selectivity for Chloridometalates over Chloride

Innis Carson,[†] Kirstian J. MacRuary,[†] Euan D. Doidge,[†] Ross J. Ellis,[†] Richard A. Grant,[‡] Ross J. Gordon,[‡] Jason B. Love,[†] Carole A. Morrison,*[,†] Gary S. Nichol,[†] Peter A. Tasker,*[,†] and A. Matthew Wilson[†]

[†]EaStCHEM School of Chemistry, University of Edinburgh, David Brewster Road, Edinburgh, EH9 3FJ, United Kingdom

[‡]Johnson Matthey Technology Centre, Sonning Common, Reading, RG4 9NH, United Kingdom

Supporting Information

ABSTRACT: High anion selectivity for $PtCl_6^{2-}$ over Cl^- is shown by a series of amidoamines, $R^1R^2NCOCH_2CH_2NR^3R^4$ (L1 with $R^1 = R^4$ = benzyl and $R^2 = R^3$ = phenyl and L3 with R^1 = H, R^2 = 2-ethylhexyl, R^3 = phenyl and R^4 = methyl), and amidoethers, $R^1R^2NCOCH_2CH_2OR^3$ (L5 with R^1 = H, R^2 = 2-ethylhexyl and R^3 = phenyl), which provide receptor sites which extract $PtCl_6^{2-}$ preferentially over Cl^- in extractions from 6 M HCl solutions. The amidoether receptor L5 was found to be a much weaker extractant for $PtCl_6^{2-}$ than its amidoamine analogues. Density functional theory calculations indicate that this is due to the difficulty in protonating the amidoether to generate a cationic receptor, LH^+, rather than the latter showing weaker binding to $PtCl_6^{2-}$. The most stable forms of the receptors, LH^+, contain a tautomer in which the added proton forms an intramolecular hydrogen bond to the amide oxygen atom to give a six-membered proton chelate. Dispersion-corrected DFT calculations appear to suggest a switch in ligand conformation for the amidoamine ligands to an open tautomer state in the complex, such that the cationic N−H or O−H groups are also readily available to form hydrogen bonds to the $PtCl_6^{2-}$ ion, in addition to the array of polarized C−H bonds. The predicted difference in energies between the proton chelate and nonchelated tautomer states for L1 is small, however, and the former is found in the X-ray crystal structure of the assembly $[(L1H)_2PtCl_6]$. The DFT calculations and the X-ray structure indicate that all LH^+ receptors present an array of polarized C−H groups to the large, charge diffuse $PtCl_6^{2-}$ anion resulting in high selectivity of extraction of $PtCl_6^{2-}$ over the large excess of chloride.

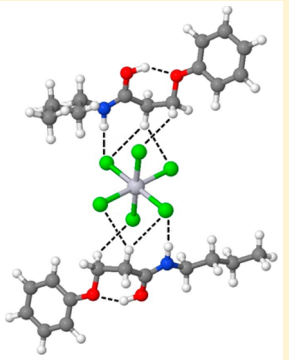

INTRODUCTION

The design of highly selective receptors for anions is of considerable current interest.[1−5] While most of the work on complexation of inorganic anions has targeted small (hard) anions such as chloride and phosphate, the design features which will discriminate in favor of larger, softer anions such as metalates is less frequently studied. An example of particular commercial importance is the provision of high selectivity for chloridometalate anions such as $PtCl_6^{2-}$ over the much smaller Cl^-. Such selectivity is essential in processes to recover platinum from aqueous solutions obtained from the oxidative leaching of minerals containing the platinum group metals (PGMs) with strong hydrochloric acid.[6−9] The kinetic inertness of the PGMs means that it is not practicable to use reagents which displace chloride ions to form inner-sphere, organic-soluble, complexes (eq 2) on the time scales used in solvent extraction processes used to recover base metals.[10]

$$2L_{org} + 2H^+_{aq} + [PtCl_6]^{2-}_{aq} \rightleftharpoons [(LH)_2PtCl_6]_{org} \quad (1)$$

$$2L_{org} + [PtCl_6]^{2-}_{aq} \rightleftharpoons [L_2PtCl_4]_{org} + 2Cl^-_{aq} \quad (2)$$

$$L_{org} + H^+_{aq} + Cl^-_{aq} \rightleftharpoons [LH.Cl]_{org} \quad (3)$$

Amines,[11] amides,[12] trialkylphosphates,[13] and phosphine oxides[14,15] have been used as solvent extractants to transport the chloridometalate intact as in the pH-dependent process shown in eq 1.[6,7,10] The extractant must show a high selectivity for the chloridometalate anion over chloride to ensure that the chloride transfer shown in eq 3 does not predominate. One approach to achieve this is to develop receptors LH^+ which have H-bond donor groups that recognize the centers of negative charge on the chloridometalate anion. Amido-functionalized tertiary amines (Figure 1) have been reported which meet this criterion, and they have indeed been found to be stronger chloridometalate extractants than the analogous unsubstituted tertiary amines.[16−22]

A feature of the amidoamine extractants (Figure 1) is that when the tertiary amine group is protonated to form the cationic receptor, they are all able to form a strong internal H-bond to a neighboring amido oxygen atom. This increases the effective basicity of the reagent and the formation of the "proton chelate" which can align an array of C−H and N−H groups to match the distribution of charge on the target

Received: June 11, 2015
Published: August 26, 2015

DOI: 10.1021/acs.inorgchem.5b01317
Inorg. Chem. 2015, 54, 8685−8692

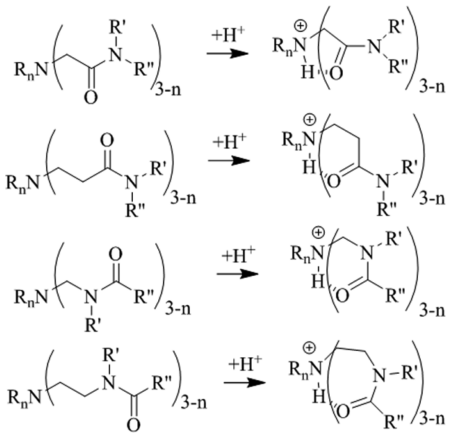

Figure 1. Tripodal amidoamines which have been used as chloridometalate extractants and the five-, six-, and seven-membered "proton chelates" which can be formed during metal extraction by the protonated reagents.

chloridometalate species.[6] This is very clearly demonstrated by the X-ray crystal structure of a $ZnCl_4^{2-}$ assembly in which the receptor site directs four polarized C−H and N−H groups toward the edges and the center of a face of the $ZnCl_4^{2-}$ tetrahedron.[18] This work examines whether structurally analogous amidoethers can function in a similar manner. A potential advantage of these latter reagents is that their lower basicity might make it easier to subsequently release the chloridometalate species, allowing them to be stripped by contacting the loaded organic phase with water, generating chloroplatinic acid as in eq 4.

$$[(LH)_2PtCl_6]_{org} \rightleftharpoons H_2PtCl_6 + 2L_{org} \quad (4)$$

To this end, a hydrocarbon-soluble amidoether reagent L5 (Figure 2) with a 2-ethylhexyl substituent at site R_2, along with

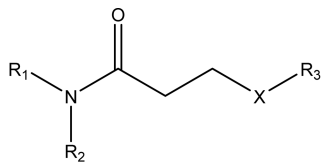

	Mode of study	R_1	R_2	X	R_3
L1	Exp + DFT	C_6H_5	$C_6H_5CH_2$	N-$CH_2C_6H_5$	C_6H_5
L2	DFT	CH_3	*n*-C_4H_9	N-CH_3	C_6H_5
L3	Exp	H	2-ethylhexyl	N-CH_3	C_6H_5
L4	DFT	H	*n*-C_4H_9	N-CH_3	C_6H_5
L5	Exp	H	2-ethylhexyl	O	C_6H_5
L6	DFT	H	*n*-C_4H_9	O	

Figure 2. Amidoamine (L1−L4) and amidoether (L5−L6) reagents discussed in this work.

two amidoamine analogues (L1 and L3) have been prepared in this work to compare their extraction properties. Density functional theory (DFT) calculations were undertaken with shorter chain, *n*-butyl analogues, L2, L4, and L6, and with the more conformationally rigid L1, which also afforded crystals of $[(L1H)_2PtCl_6]$ suitable for X-ray structure determination.

EXPERIMENTAL SECTION

All solvents and reagents were used as received from commercial suppliers. Deionized water was obtained from a Milli-Q purification system. ^1H and ^{13}C nuclear magnetic resonance (NMR) spectra were obtained on a Bruker AVA 500 or 600 spectrometer as solutions in $CDCl_3$. Chemical shifts (δ's) are reported in parts per million (ppm) relative to the residual solvent (δ_H 7.26 and δ_C 77.0). Mass spectra were recorded on a MAT 900 XP spectrometer (EI) or a Thermo-Fisher LCQ Classic (ESI). Elemental analyses were determined by Mr. Stephen Boyer at London Metropolitan University, School of Human Sciences, Science Centre, London Metropolitan University, 29 Hornsey Road, London, N7 7DD. Crystal structure data (CCDC-1406119) were collected at 150 K on a three circle Rigaku Oxford Diffraction SuperNova CCD diffractometer equipped with an Oxford Cryosystems low temperature device with Cu Kα radiation (λ = 1.541 78 Å). The new reagents L1, L3, and L5 were prepared by adaptation of methods described previously.[23]

***N*-Benzyl-3-(benzyl(phenyl)amino)-*N*-phenylpropanamide (L1).** Neat 3-bromopropanoyl chloride (18.7 g, 109 mmol) was added dropwise to a stirred solution of *N*-benzylaniline (38.5 g, 210 mmol) in CH_2Cl_2 (200 mL) at 0 °C and then stirred at room temperature for 1 h. The resulting mixture was filtered; *N*-benzylaniline (37.3 g, 204 mmol) was added to the filtrate, and the mixture refluxed for 3 h. After filtration and evaporation of solvent, the resulting oil purified on a silica column, eluting with 20% chloroform in hexane to give the title compound as a pale yellow/green oil, yield 14.5 g (32%). ^1H NMR (δ_H, 500 MHz, $CDCl_3$) 6.56−7.34 (m, 20H, aromatic H), 4.91 (s, 2H, CH_2), 4.46 (s, 2H, CH_2), 3.60 (t, 2H, CH_2), 2.50 (t, 2H, CH_2). ^{13}C NMR (δ_C, 125 MHz, $CDCl_3$) 171.2, 137.3, 129.7, 129.3, 128.9, 128.5, 128.4, 128.1, 127.4, 54.3, 53.6, 47.7, 32.0. *m*/*z* (ESI) 421.92 ($M+H^+$).

***N*-(2-Ethylhexyl)prop-2-enamide.** Neat 2-ethylhexylamine (6 mL, 37 mmol) was added dropwise to a stirred solution of acryloyl chloride (3 mL, 37 mmol) in dry CH_2Cl_2 (20 mL) at 0 °C. After stirring for 30 min at room temperature, the reaction was quenched with saturated sodium hydrogen carbonate solution (3 × 30 mL) and the organic phase washed with water (30 mL) and dried over $MgSO_4$. The solvent was evaporated under vacuum to give the title compound as a colorless oil which was used without further purification in the preparation of **L3**, yield 4.84 g (72%). ^1H NMR (δ_H, 600 MHz, $CDCl_3$) 6.29 (dd, 1H, **H**C=CH_2), 6.12 (dd, 1H, C=C**H**′H), 5.64 (dd, 1H, C=CH′**H**), 3.34−3.26 (m, 2H, CH_2NH), 1.52−1.48 (m, 1H, CH), 1.38−1.27 (m, 8H, CH and CH_2), 0.95−0.88 (m, 6H, CH_3). ^{13}C NMR (δ_C, 125 MHz, $CDCl_3$) 165.7, 131.0, 126.1, 42.5, 39.4, 31.0, 28.9, 24.3, 23.0, 14.1, 10.9.

***N*-(2-Ethylhexyl)-3-(methylphenylamino)-propanamide (L3).** A mixture of *N*-(2-ethylhexyl)prop-2-enamide (4.0 g, 22 mmol), *N*-methylaniline (2.6 g, 24 mmol), and $SiCl_4$ (2 mol %) was stirred and heated under N_2 at 70 °C for 16 h. The mixture was dissolved in CH_2Cl_2 (20 mL), washed with water (3 × 20 mL), and dried over $MgSO_4$. The solvent was removed and the crude product purified on a silica column, eluting with 10% methanol in CH_2Cl_2 to give the title compound as a pale yellow oil, yield 4.1 g (65%). ^1H NMR (δ_H, 600 MHz, $CDCl_3$) 7.28−7.26 (m, 2H, aromatic H), 6.79−6.76 (3H, aromatic H), 3.69 (t, 2H, $CH_2N(CH_3)$), 3.2 (m, 2H, CH_2NH), 2.95 (s, 3H, NCH_3), 2.44 (t, 2H, $CH_2CH_2N(CH_3)$), 1.42−1.38 (m, 1H, CH), 1.31−1.20 (m, 8H, CH_2), 0.93−0.86 (m, 6H, CH_3). ^{13}C NMR (δ_C, 151 MHz, $CDCl_3$) 171.5, 148.9, 129.3, 117.2, 113.1, 49.4, 42.4, 39.3, 38.8, 34.1, 31.0, 28.9, 24.2, 23.0, 14.1, 10.8. *m*/*z* (ESI) 290.2 ($M + H^+$).

3-Phenoxypropanoic Acid. A mixture of 3-phenyoxynitrile (9.88 g, 67 mmol) in 6 M HCl (50 mL) was heated at reflux temperature for 16 h. After being cooled, the mixture was filtered and the precipitate recrystallized from 40:60 benzene/petroleum ether (60−80 °C) to give the title compound as colorless crystals, yield 6.95 g (62%). ^1H NMR (δ_H, 500 MHz, $CDCl_3$) 7.36−7.31 (m, 2H, aromatic H), 7.06−7.02 (m, 1H, aromatic H), 6.96−6.92 (m, 1H, aromatic H), 4.23 (t, 2H, CH_2), 2.86 (t, 2H, CH_2). ^{13}C NMR (δ_C, 125 MHz, $CDCl_3$) 177.4, 158.4, 129.5, 121.2, 114.7, 63.0, 34.4.

3-Phenoxypropanoyl Chloride. A mixture of 3-phenoxypropanoic acid (5.80 g, 35 mmol) and thionyl chloride (4.5 mL, 62 mmol) was stirred at room temperature for 3 h. Excess thionyl chloride was removed by vacuum distillation to give the title compound as an orange oil which was used in the preparation of **L5** without further

DOI: 10.1021/acs.inorgchem.5b01317
Inorg. Chem. 2015, 54, 8685−8692

purification, yield 6.26 g (97%). ^{1}H NMR (δ_H, 500 MHz, $CDCl_3$) 7.44−7.35 (m, 2H, aromatic H), 7.09 (dd, 1H, aromatic H), 6.99 (d, 2H, aromatic H), 4.30 (t, 2H, CH_2), 3.36 (t, 2H, CH_2). ^{13}C NMR (δ_C, 125 MHz, $CDCl_3$) 171.7, 158.2, 129.7, 121.7, 114.8, 62.7, 46.7.

***N*-(2-Ethylhexyl)-3-phenoxypropanamide (L5).** Neat 2-ethylhexylamine (6.12 g, 47 mmol) was added dropwise to a stirred solution of 3-phenoxylpropanoyl chloride (6.07 g, 33 mmol) in dry CH_2Cl_2 (75 mL). After 3 h at room temperature, the solvent was evaporated and the resulting oil purified on a silica column eluting with 10% ethyl acetate in hexane to give the title compound as a pale yellow oil, yield 6.21 g (68%). ^{1}H NMR (δ_H, 500 MHz, $CDCl_3$) 7.32−7.25 (m, 2H, aromatic H), 6.97 (t, 2H, aromatic H), 6.90 (d, 1H, aromatic H), 6.22 (s, 1H, NH), 4.25 (t, 2H, CH_2), 3.29−3.17 (m, 2H, CH_2), 2.67 (t, 2H, CH_2), 1.49−1.40 (m, 1H, CH), 1.37−1.21 (m, 8H, CH_2), 0.95−0.83 (m, 6H, CH_3). ^{13}C NMR (δ_C, 125 MHz, $CDCl_3$) 170.7, 158.2, 129.6, 121.2, 114.5, 64.3, 42.3, 39.3, 36.9, 31.0, 28.9, 24.2, 23.0, 14.1, 10.9. *m*/*z* (ESI) 300.19 (M + Na^+). Anal. Calcd for $C_{17}H_{27}NO_2$: C 73.61, H 9.81, N 5.05. Found: C 73.71, H 9.75, N 5.09.

General Extraction Procedure. Analytical grade toluene was used as the water-immiscible solvent for the extractants and deionized water for the hexachloroplatinate solutions. Inductively coupled plasma emission spectroscopy (ICP-OES) calibration standards were prepared by dilution of commercially available standards. ICP-OES was carried out on a PerkinElmer Optima 5300 DV employing a radio frequency (RF) forward power of 1400 W, with argon gas flows of 10, 1.4, and 0.45 L min^{-1} for plasma, auxiliary, and nebulizer flows. Using a peristaltic pump, sample solutions were taken up into a Gem Tip cross-flow nebulizer and a glass cyclonic spray chamber at a rate of 2.0 mL min^{-1}. Solutions of extractants were prepared at concentrations ranging from 0.10 to 1.00 M by dilution of a 1.00 M solution in toluene. Five mL portions of these solutions were contacted with 5 mL of chloridoplatinate solution (0.01 M Pt, 6 M HCl) and stirred vigorously in sealed vials for 16 h at room temperature, after which the phases were separated and 0.5 mL aliquots of each diluted to 10 mL in 1-methoxy-2-propanol for ICP-OES analysis.

Computational Modeling. Geometry optimization calculations were carried out for L1, L2, L4 (which is a shorter chain model system for L3), and L6 (which similarly is a model system for L5) using the Gaussian 09 program.[24] No attempts were made to model solvation of assemblies. The justification for this stems from the fact that the solvation/desolvation energies in the aqueous phase are identical for all extractions, involving only H^+_{aq} and $[PtCl_6]^{2-}_{aq}$, leaving only the differences in the solvation energies of L_{org} and $[(LH)_2PtCl_6]_{org}$ arising from variations of the R and X substituents on the ligands to influence the correlation between calculated formation energies and the observed strength of extraction. In the organic phase (toluene which has a low dielectric constant), any dependence of the overall formation energy of the complex on solvation is likely to involve only the minor differences originating from variation of the R and X groups. Atom coordinates for all energy-minimized structures can be found in the Supporting Information. The B3LYP[25] exchange/correlation functional was used throughout (data reported in the Supporting Information), alongside the highly parametrized M06-2X functional[26] to assess the impact of a dispersion-corrected functional. As expected, the dispersion correction had minimal impact on ligand protonation energies (Table 2 and Table S1, Supporting Information), but a marked impact on their binding energies (due to the prevalence of soft C−H···Cl) and complex formation energies (Table 3 and Table S2, Supporting Information). The 6-31+G(d) basis set was applied to all atoms with the exception of platinum, for which the LANL2DZ pseudopotential/basis set was used. Structures were considered optimized when the forces and atomic displacements fell to within the program default convergence criteria. Assembly formation energies and protonation energies were calculated using the difference in internal energy values of the sum of the products and the sum of the individual reactants (corrected for basis set superposition error using the Counterpoise correction method).[27,28] Natural bond order (NBO) analysis, which uses "Lewis"-type orbitals to describe donor and acceptor orbitals and their interactions, was performed using NBO 6.0[29] on optimized structures in a similar manner to that used by Turkington et al.[20] *In vacuo* classical molecular dynamics (MD) simulations were employed to investigate the possible formation of larger assemblies of L1 and $PtCl_6^{2-}$. These were performed using the OPLS-AA[30] force field with the software package LAMMPS.[31] An initial model, comprising two $L1H^+$, two LH, and one $PtCl_6^{2-}$ entities randomly distributed in a cubic simulation cell of length 40 Å, was constructed using Packmol.[32] The integration time step was set to 1 fs, and time increments accrued using the standard Velocity-Verlet algorithm. Aggregation of all species to create a $[(L1H)_2\{(L1H)Cl\}_2PtCl_6]$ system occurred very quickly (within 30 ps); in total, system dynamics were accrued for 10 200 ps, which included 500 ps equilibration time. The simulation was run under canonical (NVT) ensemble conditions (with the temperature thermostated at room temperature using the Nosé−Hoover thermostat system); the potential energy values obtained during the production run were collected and then averaged.

RESULTS AND DISCUSSION

The uptake of $PtCl_6^{2-}$ from 6 M aqueous HCl by toluene solutions containing varying concentrations of the amidoamine reagents L1 or L3 or the amidoether reagent L5 (Figure 3)

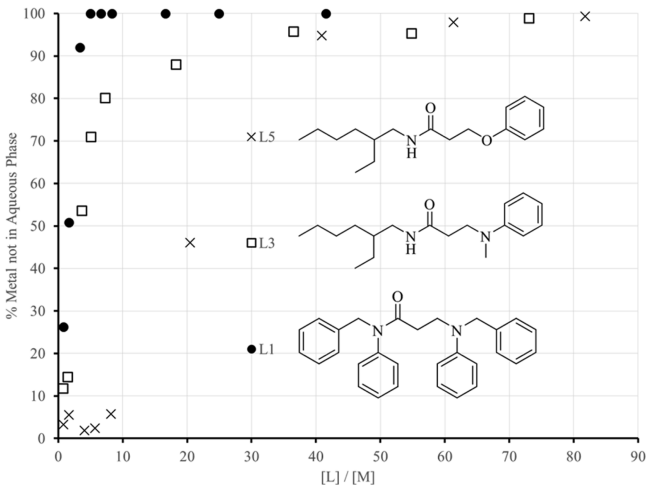

Figure 3. Pt recovery from aqueous solutions of 0.01 M H_2PtCl_6 in 6 M HCl by equal volumes of toluene solutions of L1, L3, and L5 as a function of extractant concentration.

indicates that L1 and L3 are stronger extractants, requiring lower L:Pt molar ratios to remove >90% of $PtCl_6^{2-}$ from the aqueous phase. The formation of a third phase that was not soluble in either the bulk toluene or aqueous phases, was observed for all of the extractions undertaken, but the material balances were good with the loss of $PtCl_6^{2-}$ from the aqueous phase being equal to that detected in the toluene and the third phase.

In order to define the origins of the greater extractant strength of the amidoamines L1 and L3 over their amidoether analogue, L5, DFT calculations were carried out to compare the ease of protonation (ΔU_p) to generate the active forms (eq 5) and to compare the binding energies (ΔU_b's) of these to the $PtCl_6^{2-}$ dianion (eq 6). The overall formation energies (ΔU_f's) of the neutral assemblies $[(LH)_2PtCl_6]$ for the reaction shown in eq 7 represent the gas-phase equivalents of the solvent extraction process shown in eq 1. In order to make valid comparisons of these energies of reaction it is essential that the lowest energy forms of the various entities shown in eqs 5−7 are used in the calculations. To reduce the numbers of conformers of the 2-ethylhexyl groups in L3 and L5 which will

DOI: 10.1021/acs.inorgchem.5b01317
Inorg. Chem. 2015, 54, 8685−8692

Table 1. Energies of Formation of Tautomers of Each of the Protonated Amidoamines $L1H^+$, $L2H^+$, $L4H^+$, and Amidoether $L6H^+$, Derived from Equation 5 Using the M06-2X/6-31+G(d)/LANL2DZ Level of Theory[a]

	Structure of protonated amidoamine	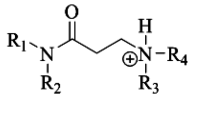	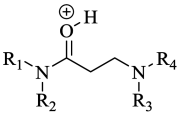	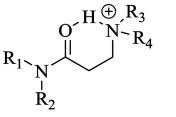
Protonation ΔU energy/kJ mol^{-1}	$L1H^+$	-281.9	-254.5	-325.7
	$L2H^+$	-267.7	-233.6	-319.7
	$L4H^+$	-238.0	-172.9	-295.9
	Structure of protonated amidoether	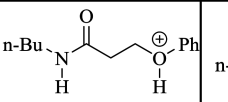	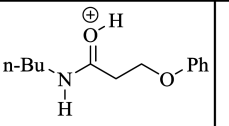	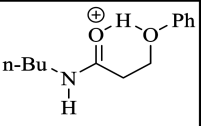
Protonation ΔU energy/kJ mol^{-1}	$L6H^+$	-83.1	-161.6	-222.9

[a]Note that for L4 and L6 energies are quoted relative to the more stable dimeric forms of the unprotonated reagents.

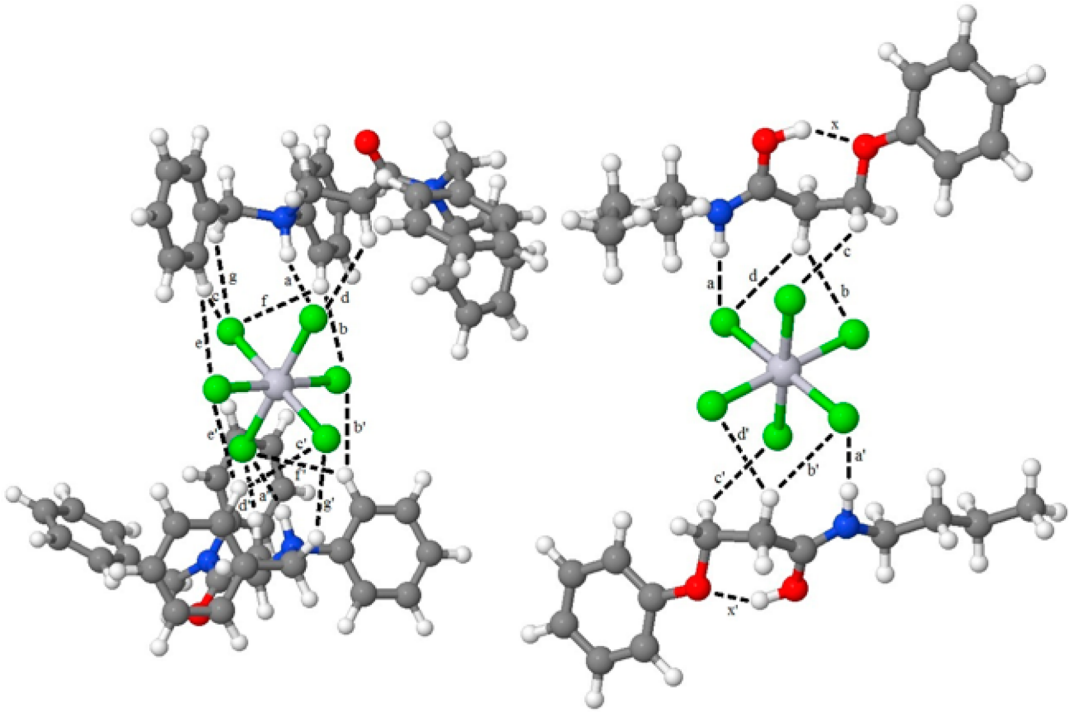

Figure 4. Lowest energy calculated structures of $[(L1H)_2PtCl_6]$ (left) and $[(L6H)_2PtCl_6]$ (right). The contacts a–g and a′–g′ shown have Natural Bond Order (NBO) energies ≥5 kJ mol^{-1} (Figures S2 and S9, respectively, Supporting Information).

have very similar energies, the *n*-butyl analogues L4 and L6 were used as model systems in the DFT calculations. L2 was used as a less rigid analogue of L1 to allow comparisons of tertiary amides with the secondary amides L4 and L6.

$$L + H_3O^+ \rightleftharpoons LH^+ + H_2O \quad (5)$$

$$2LH^+ + PtCl_6^{2-} \rightleftharpoons [(LH)_2PtCl_6] \quad (6)$$

$$2L + 2H_3O^+ + PtCl_6^{2-} \rightleftharpoons [(LH)_2PtCl_6] + 2H_2O \quad (7)$$

Interesting issues arise when identifying the most stable gas-phase structures and when considering whether similar structures are likely to be the most stable forms in toluene, which was used in the solvent extraction experiments. The unprotonated reagents that contain secondary amide groups (i.e., R_1 = H) associate to form dimers, such that L4 and L6 form $(L4)_2$ and $(L6)_2$, which are more stable than the intramolecular H-bonded monomers of L4 and L6, with energies of dimerization of −29.4 and −30.1 kJ mol^{-1}, respectively (Figure S1 in Supporting Information). In contrast,

DOI: 10.1021/acs.inorgchem.5b01317
Inorg. Chem. 2015, 54, 8685−8692

the tertiary amide reagents L1 and L2, which have no amido N−H, show no propensity for dimerization.

Protonation of the reagents can give rise to a number of different structures, the stabilities of which are dependent upon which functional group is protonated and whether or not an intramolecular H-bond is formed. For the amidoamines it was found in all cases that protonation of the amine nitrogen gave rise to more stable structures than those protonated at the carbonyl oxygen (Table 1). For the amidoether (L6), protonation at the carbonyl oxygen is preferred to that at the ether group. Protonation energies are more favorable for amidoamines than for the amidoether, which can be attributed to the higher basicity of the amine. Note that the protonation energy for L4 is less favorable than those for L1 and L2 because the lowest energy state for L4 was taken to be the dimer $(L4)_2$ and two H-bonds in the dimerized form have to be broken to generate $L4H^+$ (Figure S1, Supporting Information). Also, the "proton chelate" form, with an internal H-bond, was found to be the global minimum conformation for all ligand systems.

Geometry optimizations to yield the lowest energy forms of the $[(LH)_2PtCl_6]$ assemblies at the M06-2X/6-31+G(d)/LANL2DZ level contained, in the cases of amidoamines L1, L2, and L4, the tautomer of the receptor which lacks a "chelated proton" (first column, Table 1). As a consequence, the cationic N−H or O−H groups are readily available to form H-bonds to the $PtCl_6^{2-}$ ion, as well as an array of polarized C−H bonds (see Figure 4, right). Note that at the B3LYP/6-31+G(d)/LANL2DZ lower level of theory (given in the Supporting Information) the proton chelate form was the lower energy state in all cases, highlighting that the balance between internal hydrogen bond versus C−H···Cl can be tipped when an improved description of dispersion interactions is introduced. In contrast, a different behavior appears to be exhibited by the amidoether L6. In the $[(L6H)_2PtCl_6]$ assembly, the $L6H^+$ still retains the "proton chelated" conformation it preferentially adopts in isolation (Table 1), with the proton formally residing on the carbonyl oxygen atom of the amide. This renders the amido N−H group in L6 cationic, allowing it to form a very strong interaction with $PtCl_6^{2-}$ (Figure 4, right).

In the case of $[(L4H)_2PtCl_6]$, the nonchelated form of the receptor is particularly strongly preferred, with the chelated form 46.9 kJ mol^{-1} higher in energy (see Table 2, and the right and left images of Figure 5, respectively). This arises because the nonchelated form can use both the amido NH and the ammonium $^+$NH units to interact with the anion, leading to a slightly stronger binding energy (see below and Supporting Information Figures S6 and S7). The lack of similar behavior in the case of $[(L6H)_2PtCl_6]$ is presumably due to the instability of the form of $L6H^+$ with the proton residing formally on the ether oxygen atom (see Table 1).

All the energy-minimized structures of the $[(LH)_2PtCl_6]$ assemblies have several polarized C−H bonds forming bonding interactions with the $PtCl_6^{2-}$ anion (Figures S2−S9, Supporting Information). A similar feature is found in the solid-state structure of $[(L1H)_2PtCl_6]$ (Figure 6), crystals of which were isolated by diffusion of diethyl ether into a methanol solution of the third phase formed during the solvent extraction experiment. The solid-state structure shows that the proton which has been added to generate the cationic receptor $L1H^+$ is sited on the benzylamine nitrogen atom N and is strongly hydrogen bonded to the amido oxygen atom O (N−H···O = 1.86(4) or 1.90(3) Å) to form the six-membered "proton chelate". This is in contrast to the nonchelated assembly structure which was calculated to be lower in energy, though as the calculated difference in energy between the two structures is small (9.1 kJ mol^{-1}, see Table 2) it is not surprising that the proton chelated structure could exist. Further weak interactions are formed with C−H bonds from two other L1 units in the solid state (lower part of Figure 6). This suggests that the aryl groups in L1 are not large enough to create a sufficiently hydrophobic exterior in a 2:1 assembly with a $PtCl_6^{2-}$ dianion, and so may not be able to ensure high solubility in toluene. This may account for the formation of a third phase in the extraction experiments.

Table 2. Energies of Formation (M06-2X/6-31+G(d)/LANL2DZ), ΔU_f, of the $[(LH)_2PtCl_6]$ Assemblies Containing the Proton Chelated and Nonchelated Tautomers of L1, L3, L4, and L6; the Protonation Energies (ΔU_p's) Required To Generate the Most Stable Form of these Cations, LH^+, and Their Binding Energies (ΔU_b) to $PtCl_6^{2-}$

reagent	structure of protonated ligand	ΔU_p/kJ mol^{-1}	ΔU_b/kJ mol^{-1}	ΔU_f[a]/kJ mol^{-1}
L1	chelated proton	−325.7	−917.6	−1569.0
	nonchelated tautomer	−325.7	−925.7	−1577.1
L2	chelated proton	−319.7	−916.4	−1555.9
	nonchelated tautomer	−319.7	−946.0	−1585.4
L4	chelated proton	−295.9	−940.8	−1532.6
	nonchelated tautomer	−295.9	−987.7	−1579.5
L6	chelated proton	−222.9	−1044.2	−1490.1
	nonchelated tautomer	−222.9	−884.8	−1330.7

[a] $\Delta U_f = 2\Delta U_p + \Delta U_b$.

Formation energies, ΔU_f's, for the most stable forms of the $[(LH)_2PtCl_6]$ assemblies were determined, along with protonation energies (ΔU_p's) and binding energies (ΔU_b's) to $PtCl_6^{2-}$ (Table 2). In accordance with the empirical extraction data (Figure 3), which show the amidoether ligand L5 to be the weakest extractant, the formation energy for the $[(LH)_2PtCl_6]$ assembly for the amidoether model system L6 is calculated to be the least favorable. The formation energy is dependent on both the protonation and binding energies, and it is apparent that the lower formation energy for $[(L6H)_2PtCl_6]$ can be attributed to L6 having the least favorable protonation energy; the corresponding binding energy for this ligand is actually the most favorable of the ligand set. For the amidoamines L1, L2, and L4 the formation energies are broadly similar and thus offer no clear prediction as to whether secondary or tertiary amides will be the stronger extractants. While differences in binding energies are apparent, they are offset by corresponding differences in protonation energies, such that while the secondary amide L4 has the most favorable binding energy for the amidoamines (a consequence of the presence of the strongly H-bonding amido N−H group), this is countered by the least favorable protonation energy.

In a prediction of whether or not a particular reagent will be a strong platinum extractant, the selectivity of the receptor for $PtCl_6^{2-}$ over Cl^- is an important factor because the extraction processes are competitive (see eqs 1 and 3) and Cl^- will be present in large excess in the aqueous solutions which contain high concentrations of HCl (the data presented in Figure 3 relate to 6 M HCl). As such, in order to compare metalate

DOI: 10.1021/acs.inorgchem.5b01317
Inorg. Chem. 2015, 54, 8685−8692

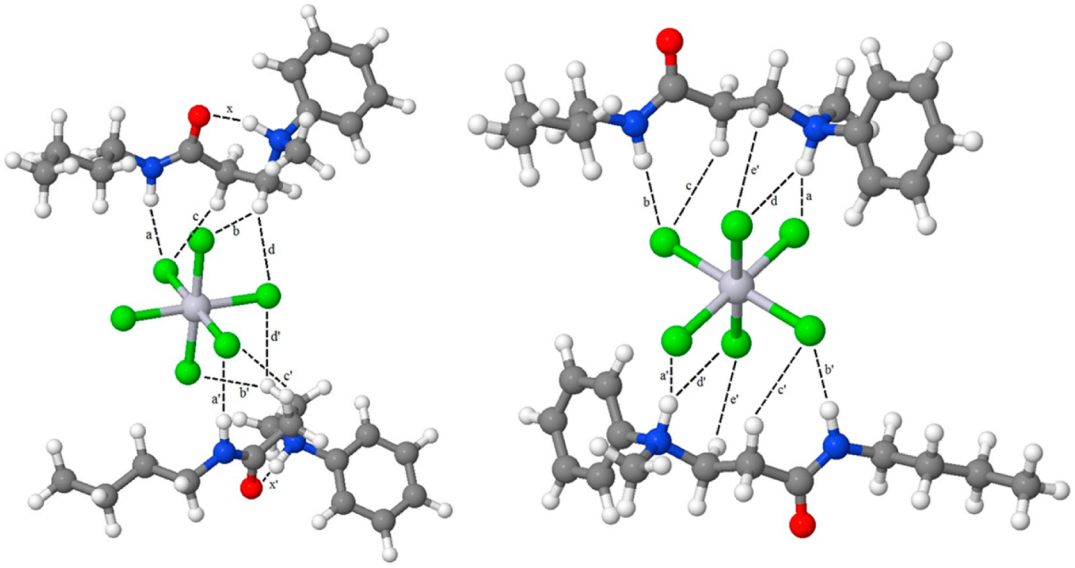

Figure 5. Energy-minimized structures of $[(L4H)_2PtCl_6]$ with $L4H^+$ units input in the "chelate-proton" conformer (left) and a "nonchelated" conformer (right). The contacts shown have NBO energies ≥5 kJ mol^{-1} (Figure S6 and S7, Supporting Information).

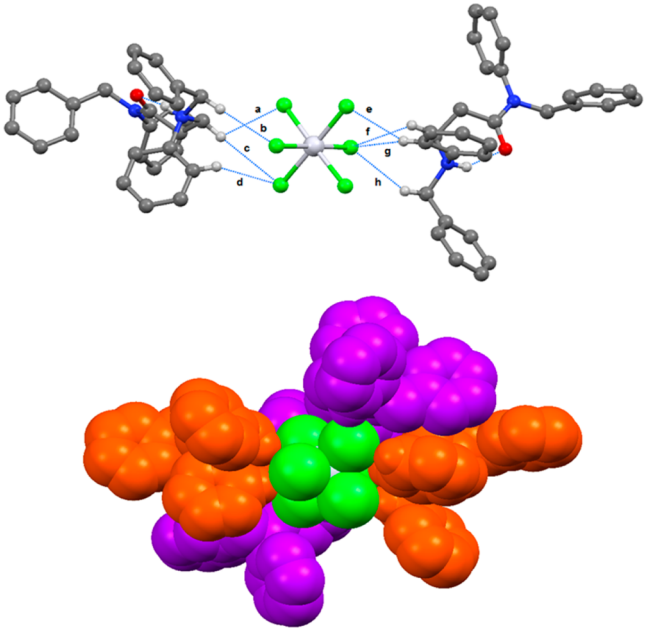

Figure 6. Solid-state structure of $[(L1H)_2PtCl_6]$ with Cl, O, and N atoms in green, red, and blue, showing contacts between ligand C−H groups and $PtCl_6^{2-}$ (a, 2.938; b, 2.933; c, 3.210; d, 2.946; e, 2.814; f, 2.947; g, 2.883; h, 2.861 Å) comparable to those in the energy-minimized structure (Figure 4) and a space-filling representation showing the approach of two further $L1H^+$ units (purple) from neighboring $[(L1H)_2PtCl_6]$ assemblies.

versus chloride, the energies of formation of the ion pairs LH^+Cl^- (ΔU_{fCl}, see eq 8) were calculated (Table 3). In all cases, the most stable form of the ion pair has a close contact between the N−H bond of the protonated amine and the chloride ion (Figure 7), which is consistent with the latter being a "hard" anion and the N−H unit being a good H-bond donor. The energies of the gas-phase ion exchange reactions, ΔU_{ex}'s, derived by eq 9, were also calculated (Table 3). The negative values determined in each case indicate that formation of the chloridoplatinate assembly, rather than the chloride ion pair, is

Table 3. Energies of Formation (M06-2X/6-31+G(d)/LANL2DZ) of the Ion Pairs [(LH)Cl] from the Most Stable Forms of L1, L2, L4, and L6 (ΔU_{fCl}); the Protonation Energies (ΔU_p) Associated with Forming the Most Stable Form of the Cations LH^+; Their Binding Energies (ΔU_{bCl}) to Cl^-; and the Energies of the Gas-Phase Ion Exchange Reaction As Expressed by Equation 9[a]

	ΔU_p /kJ mol^{-1}	binding energy, ΔU_{bCl}/kJ mol^{-1}	overall formation energy, ΔU_{fCl} /kJ mol^{-1}	energy of anion exchange reaction, ΔU_{ex}/kJ mol^{-1}
L1	−325.7	−409.0	−734.6	−107.8
L2	−319.7	−412.6	−732.3	−120.8
L4	−295.9	−428.5	−724.4	−130.7
L6	−222.9	−433.1	−659.1	−177.9

[a] $\Delta U_{ex} = \Delta U_f - 2\Delta U_{fCl}$.

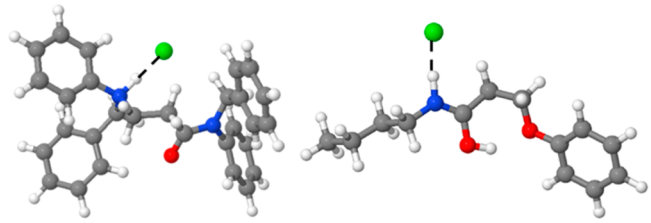

Figure 7. Energy-minimized structures of the ion pairs, LH^+Cl^-, formed by L1 (left) and L6 (right).

favored for all ligand systems. This information helps to account for the observation that in solvent extraction processes significant uptake of $PtCl_6^{2-}$ is observed from aqueous solutions even in the presence of a large excess of chloride ions.[6]

A feature of the ligands discussed in this work is that they present an array of polarized N−H and C−H bonds which favor formation of assemblies with the larger, charge diffuse, $PtCl_6^{2-}$ ion, rather than the smaller "hard" chloride ion. It is clear from estimates of the energies of the interaction of the LH^+ cations with $PtCl_6^{2-}$ (Figures S2 and S3, Supporting Information) that N−H···$PtCl_6^{2-}$ bonding is much stronger

DOI: 10.1021/acs.inorgchem.5b01317
Inorg. Chem. 2015, 54, 8685−8692

than C−H···$PtCl_6^{2-}$ bonding. However, when the preorganized form of a LH^+ receptor provides several polarized C−H units they make a significant contribution to the binding of the anion. This is substantiated by significantly higher NBO energies for the 14 C−H···Cl contacts a−g and a′−g′ in $[(L1H)_2PtCl_6]$ (Figure 4 and Figure S2, Supporting Information) compared to the conventional hydrogen bonding interactions from the $^+$NH groups in the isomeric forms of $[(L1H)_2PtCl_6]$ (Figure S3, Supporting Information) which have $L1H^+$ in a nonchelated tautomeric form.

$$LH^+ + Cl^- \rightleftharpoons [(LH)Cl] \quad (8)$$

$$2[(LH)Cl] + PtCl_6^{2-} \rightleftharpoons [(LH)_2PtCl_6] + 2Cl^- \quad (9)$$

While the DFT calculations above provide insight into the origins of the strength and selectivity of the amidoamine and amidoether extractants, it is clear that they do not completely reproduce the observed order of extractant strength, as the experimental data demonstrate that L1 is a significantly better extractant than L3, which in turn is significantly better than L5; this trend is only partly borne out by the ΔU_f values (Table 2), which show that the formation energy of L1 almost has parity with that of L4 (the model system for L3), which in turn has a higher formation energy than L6 (the model system for L5). A possible reason for this disparity is that the $[(LH)_2PtCl_6]$ assembly that was used as a basis for the DFT modeling work is not an accurate representation of those that form in the water-immiscible phases. From the X-ray crystal structure of $[(L1H)_2PtCl_6]$ (Figure 6) and the analogous energy-minimized structures (Figures 4 and 5) it is clear that there is sufficient space around the $PtCl_6^{2-}$ to accommodate further ligands, and indeed, 100% Pt-loading in extraction requires extractant to platinum ratios greater than 2:1 (Figure 3). Investigation of the formation of such large structures using quantum mechanical computational methods is impractical because of the large number of atoms involved. Moreover, the many degrees of freedom that such a large system comprises (many of which will relate to low energy torsional motions) render the concept of a global minimum energy structure less relevant. Instead a collective ensemble of low energy states, such as can be obtained from a molecular dynamics simulation, becomes a more appropriate representation. Preliminary results of *in vacuo* simulations indicate that the potential energy of the system involving association of a $PtCl_6^{2-}$ ion with two $L1H^+$ cations and two (L1H)Cl ion pairs is 209.3 ± 121.8 kJ mol^{-1} lower than the combined potential energies of one $[(L1H)_2PtCl_6]$ unit and two (L1H)Cl units (Figure 8). From this it is clear that a $PtCl_6^{2-}$ ion can readily accommodate the interactions with four L1-type ligands. An atomistic model of this type may also provide an explanation for the formation of a third phase in the extraction process because aggregation of multiple units is likely to lead to gel-like structures.

CONCLUSIONS

The protonated forms of L1−L6 have been shown to be good receptors for the $PtCl_6^{2-}$ anion. Computational work and X-ray structure determination reveal that an important feature of the anion-binding sites is the presence of an array of polarized C−H bonds that effectively address the diffuse negative charge on the chloridoplatinate ion, helping the extractants L1, L3, and L5 to show selectivity for the metalate over chloride which is present in large excess. The higher strengths of the amidoamine extractant receptors L1 and L3 as compared to that of the amidoether L5 can be ascribed to their greater basicity, making formation of the cationic receptors LH^+ more favorable. As in other areas of anion receptor design, the benefits of incorporating amide units as strong hydrogen bond donors can be offset by their propensity to bond to each other, and it is of considerable practical significance that the tertiary amide L1, which has no amido N−H unit, is a strong extractant. In contrast to the extraction of tetrahedral $ZnCl_4^{2-}$ dianions where relatively simple aminoamides[5] confer good solubility of $[(LH)_2ZnCl_4]$ assemblies in hydrocarbon solvents, the extraction of $PtCl_6^{2-}$ is characterized by formation of a third phase which could possibly contain additional extractant molecules in the form of their hydrochloride salts. Computational techniques to model the formation of the relatively large assemblies such as $[(LH)_4(PtCl_6)Cl_2]$ are in progress.

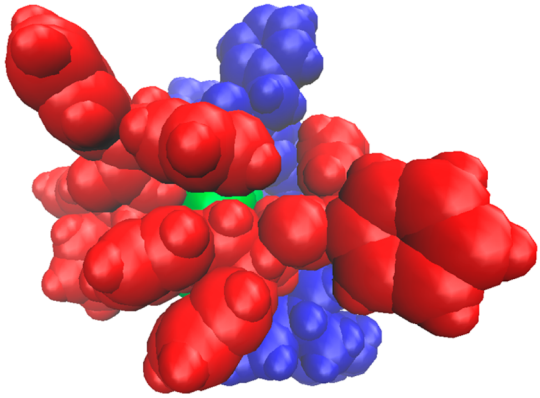

Figure 8. Space filling representation of the energy-minimized structure of $[(L1H)_2\{(L1H)Cl\}_2PtCl_6]$ assembly showing the two $L1H^+$ cations in red, the two (L1H)Cl ion pairs in blue, and the $PtCl_6^{2-}$ in green.

ASSOCIATED CONTENT

Supporting Information

The Supporting Information is available free of charge on the ACS Publications website at DOI: 10.1021/acs.inorgchem.5b01317.

Tables of energies and figures showing energy-minimized structures and NBO energies (PDF)

AUTHOR INFORMATION

Corresponding Authors

*E-mail: c.morrison@ed.ac.uk. Phone: 0131 650 4725.
*E-mail: P.A.Tasker@ed.ac.uk.

Author Contributions

The manuscript was written through contributions of all authors. All authors have given approval to the final version of the manuscript.

Notes

The authors declare no competing financial interest.

ACKNOWLEDGMENTS

We thank the EPSRC, Johnson Matthey, and The University of Edinburgh for funding for Ph.D. studentships for K.J.M., I.C., E.D.D., and A.M.W., and EaStCHEM for access to the Research Computing Facility.

DOI: 10.1021/acs.inorgchem.5b01317
Inorg. Chem. 2015, 54, 8685−8692

REFERENCES

(1) Busschaert, N.; Caltagirone, C.; Van Rossom, W.; Gale, P. A. *Chem. Rev.* **2015**, *115*, 8038.
(2) Dalla Cort, A. *Ion-Pair Receptors. Supermolecular Chemistry: From Molecules to Nanomaterials*; Wiley: New York, 2012 10.1002/9780470661345.smc068.
(3) Gale, P. A.; Caltagirone, C. *Chem. Soc. Rev.* **2015**, *44*, 4212−4227.
(4) Kim, D. S.; Sessler, J. L. *Chem. Soc. Rev.* **2015**, *44*, 532−546.
(5) Jentzsch, A. V. *Pure Appl. Chem.* **2015**, *87*, 15−41.
(6) Turkington, J. R.; Bailey, P. J.; Love, J. B.; Wilson, A. M.; Tasker, P. A. *Chem. Commun.* **2013**, *49*, 1891−1900.
(7) Grant, R. A.; Gordon, R. J.; Woolham, S. F. *International Solvent Extraction Conference*; Würzburg, Sept 7−11, 2014.
(8) Reedijk, J. *Platinum Met. Rev.* **2008**, *52*, 2−11.
(9) Bernardis, F. L.; Grant, R. A.; Sherrington, D. C. *React. Funct. Polym.* **2005**, *65*, 205−217.
(10) Wilson, A. M.; Bailey, P. J.; Tasker, P. A.; Turkington, J. R.; Grant, R. A.; Love, J. B. *Chem. Soc. Rev.* **2014**, *43*, 123−135.
(11) Ivanova, S. N.; Gindin, L. M.; Mironova, L. Y. *Izvestiya Sibirskogo Otdeleniya Akademii Naul SSSR, Seriya Khimicheskikh Nauk* **1964**, *2*, 35−43.
(12) Pohlandt, C.; Fritz, J. S. *Talanta* **1979**, *26* (5), 395−399.
(13) Berg, E. W.; Senn, W. L., Jr. *Anal. Chim. Acta* **1958**, *19*, 12−17.
(14) Knothe, M. *Z. Anorg. Allg. Chem.* **1980**, *470*, 216−226.
(15) Mhaske, A. A.; Dhadke, P. M. *J. Chem. Eng. Jpn.* **2001**, *34* (8), 1052−1055.
(16) Warr, R. J.; Westra, A. N.; Bell, K. J.; Chartres, J.; Ellis, R.; Tong, C.; Simmance, T. G.; Gadzhieva, G.; Blake, A. J.; Tasker, P. A.; Schröder, M. *Chem. - Eur. J.* **2009**, *15*, 4836−4850.
(17) Bell, K. J.; Westra, A. N.; Warr, R. J.; Chartres, J.; Ellis, R.; Tong, C. C.; Blake, A. J.; Tasker, P. A.; Schröder, M. *Angew. Chem., Int. Ed.* **2008**, *47*, 1745−1748.
(18) Ellis, R. J.; Chartres, J.; Henderson, D. K.; Cabot, R.; Richardson, P. R.; White, F. J.; Schröder, M.; Turkington, J. R.; Tasker, P. A.; Sole, K. C. *Chem. - Eur. J.* **2012**, *18*, 7715−7728.
(19) Ellis, R. J.; Chartres, J.; Tasker, P. A.; Sole, K. C. *Solvent Extr. Ion Exch.* **2011**, *29*, 657−672.
(20) Turkington, J. R.; Cocalia, V.; Kendall, K.; Morrison, C. A.; Richardson, P.; Sassi, T.; Tasker, P. A.; Bailey, P. J.; Sole, K. C. *Inorg. Chem.* **2012**, *51*, 12805−12819.
(21) Narita, H.; Morisaku, K.; Tanaka, M.; Nagao, K.; Fuchikami, T.; Yoshida, T.; Kuroda, K. *International Solvent Extraction Conference*; Sept 7−11, 2014.
(22) Narita, H.; Morisaku, K.; Mikiya, T. *Solvent Extr. Ion Exch.* **2015**, *33*, 407−417.
(23) Al-Awadi, S. A.; Abdallah, M. R.; Dib, H. H.; Ibrahim, M. R.; Al-Awadi, N. A.; El-Dusouqui, O. M. E. *Tetrahedron* **2005**, *61*, 5769−5777.
(24) *Gaussian 09, Revision D.01*; Gaussian, Inc.: Wallingford CT, 2009. Full citation available in the Supporting Information.
(25) Becke, A. D. *J. Chem. Phys.* **1993**, *98*, 5648−52.
(26) Zhao, Y.; Truhlar, D. G. *Theor. Chem. Acc.* **2008**, *120*, 215−41.
(27) Boys, S. F.; Bernardi, F. *Mol. Phys.* **1970**, *19*, 553−566.
(28) Simon, S.; Duran, M.; Dannenberg, J. J. *J. Chem. Phys.* **1996**, *105*, 11024−11031.
(29) *NBO 6.0*; Glendening, E. D.; Badenhoop, J. K.; Reed, A. E; Carpenter, J. E.; Bohmann, J. A.; Morales, C. M,; Landis, C. R.; Weinhold, F. Theoretical Chemistry Institute, University of Wisconsin: Madison, WI, 2013.
(30) Jorgenson, W. L.; Maxwell, D. S.; Tirado-Raves, J. *J. Am. Chem. Soc.* **1996**, *118*, 11225−11236.
(31) Plimpton, S. *J. Comput. Phys.* **1995**, *117*, 1−19.
(32) Martínez, L.; Andrade, R.; Birgin, E. G.; Martínez, J. M. *J. Comput. Chem.* **2009**, *30*, 2157−2164.

DOI: 10.1021/acs.inorgchem.5b01317
Inorg. Chem. 2015, 54, 8685−8692